Mon. Not. R. Astron. Soc. **379,** L25–L29 (2007) doi:10.1111/j.1745-3933.2007.00327.x

The colour selection of distant galaxies in the UKIDSS Ultra Deep Survey Early Data Release

K. P. Lane,[1⋆] O. Almaini,[1] S. Foucaud,[1] C. Simpson,[2] Ian Smail[3], R. J. McLure,[4] C. J. Conselice,[1] M. Cirasuolo,[4] M. J. Page,[5] J. S. Dunlop,[4] P. Hirst,[6] M. G. Watson[7] and K. Sekiguchi[8]

[1]*School of Physics and Astronomy, The University of Nottingham, University Park, Nottingham NG7 2RD*
[2]*Astrophysics Research Institute, Liverpool John Moores University, Twelve Quays House, Egerton Wharf, Birkenhead CH41 1LD*
[3]*Institute for Computational Cosmology, Department of Physics, Durham University, Durham DH1 3LE*
[4]*SUPA,† Institute for Astronomy, University of Edinburgh, Royal Observatory, Blackford Hill, Edinburgh EH9 3HJ*
[5]*Mullard Space Science Laboratory, University College London, Holmbury St Mary, Dorking, Surrey RH5 6NT*
[6]*Gemini Observatory Northern Operations Center, 670 N. A'ohōokōu Place Hilo, Hawaii 96720, USA*
[7]*Department of Physics & Astronomy, University of Leicester, Leicester LE1 7RH*
[8]*Subaru Telescope, National Astronomical Observatory of Japan, 650 North A'ohōokōu Place, Hilo, Hawaii 96720, USA*

Accepted 2007 April 13. Received 2007 April 12; in original form 2006 September 15

ABSTRACT

We investigate colour selection techniques for high-redshift galaxies in the UKIRT Infrared Deep Sky Survey (UKIDSS) Ultra Deep Survey Early Data Release (UDS EDR). Combined with very deep Subaru optical photometry, the depth ($K_{AB} = 22.5$) and area (0.62 deg^2) of the UDS EDR allow us to investigate optical/near-infrared selection using a large sample of over 30 000 objects. By using the $B - z'$, $z' - K$ colour–colour diagram (the BzK technique) we identify over 7500 candidate galaxies at $z > 1.4$, which can be further separated into passive and star-forming systems (pBzKs and sBzKs respectively). Our unique sample allows us to identify a new feature not previously seen in BzK diagrams, consistent with the passively evolving track of early-type galaxies at $z < 1.4$. We also compare the BzK technique with the $R - K$ colour selection of extremely red objects (EROs) and the $J - K$ selection of distant red galaxies (DRGs), and quantify the overlap between these populations. We find that the majority of DRGs at these relatively bright magnitudes are also EROs. Since previous studies have found that DRGs at these magnitudes have redshifts of $z \sim 1$, we determine that these DRGs/EROs have spectral energy distributions consistent with being dusty star-forming galaxies or active galactic nuclei at $z < 2$. Finally, we observe a flattening in the number counts of pBzK galaxies, similar to other studies, which may indicate that we are sampling the luminosity function of passive $z > 1$ galaxies over a narrow redshift range.

Key words: galaxies: evolution – galaxies: formation.

1 INTRODUCTION

Colour selection can provide an efficient technique to identify high-redshift galaxies based on known rest-frame spectral energy distribution (SED) features. However, most of these colour criteria are sensitive to more than one type of SED feature, i.e. more than one galaxy type and at potentially different redshifts.

Extremely red objects (EROs) are one class of colour-selected galaxies; these are consistent with either dust-reddened star-forming galaxies or passive galaxies at $z > 1$ (e.g. Cimatti et al. 2002; Roche et al. 2002; Simpson et al. 2006). Extending these techniques to higher redshifts, Daddi et al. (2004) suggested a more refined criterion based on two colour cuts in $B - z'$ and $z' - K$, now known as the BzK technique, where $BzK \equiv (z' - K)_{AB} - (B - z')_{AB}$. Star-forming galaxies in the range $1.4 < z < 2.5$ are selected by requiring $BzK \geqslant -0.2$. This was determined by analysing the BzK properties of $z > 1.4$ star-forming galaxies, classified through [O II] emission and ultraviolet spectra. Passive galaxies in the same redshift range require $BzK < -0.2$ and $(z' - K)_{AB} > 2.5$. This was determined by analysing the BzK properties of spectroscopically confirmed passive galaxies at $z > 1.4$. Star-forming and passive BzK galaxies will now be referred to as sBzKs and pBzKs respectively. Finally, the selection of galaxies using near-infrared colours $(J - K)_{AB} > 1.3$ (distant red galaxies, DRGs) has been shown to be an effective

⋆E-mail: ppxkl@nottingham.ac.uk
†Scottish Universities Physics Alliance.

© 2007 The Authors. Journal compilation © 2007 RAS

technique for selecting galaxies out to $z > 2$ based on the Balmer break (Franx et al. 2003).

The effectiveness of these various photometric techniques, however, is still unquantified, due in part to the small sample sizes, or shallow depths, used in previous follow-up studies. The latest generation of large-area, deep near-infrared surveys, such as the UKIRT Infrared Deep Sky Survey (UKIDSS) Ultra Deep Survey (UDS), now provide a representative sample of colour-selected sources. These can be used to determine the proportions of galaxy types selected using different colour criteria, their redshift ranges and the overlaps between different techniques.

Throughout this Letter we use a concordance cosmology with $\Omega_{\rm m} = 0.3$, $\Omega_\Lambda = 0.7$ and $H_0 = 70$ km s^{-1}Mpc^{-1}. The magnitudes and colours quoted above are based on 2 arcsec diameter aperture magnitudes, as are all magnitudes and colours quoted throughout this Letter.

2 COLOUR SELECTION OF HIGH-z GALAXIES

2.1 Data set and sample definitions

The UKIDSS has been running since the spring of 2005 and comprises five sub-surveys covering different areas and depths (Lawrence et al. 2006). The UKIDSS uses the Wide-Field Camera (Casali et al. 2007) on the United Kingdom Infrared Telescope (UKIRT). This study makes extensive use of *J*- and *K*-band data from the UDS Early Data Release (the UDS EDR; see Dye et al. 2006). The UDS is the deepest of the five UKIDSS sub-surveys and aims to reach a final depth of $K_{AB} = 25.0$, $H_{AB} = 25.4$, $J_{AB} = 26.0$ (5σ, point source) over an area of 0.8 deg^2. The size of the UDS field significantly reduces the effects of cosmic variance and on this scale the UDS will be the deepest image ever produced, providing an unparalleled number of candidate high-redshift sources. Owing to a small change in the UDS field centre shortly after the beginning of the survey, the current *JK* imaging is not uniform over the entire 0.8-deg^2 field. Consequently, for the purposes of this Letter, we restrict our analysis to the 0.62-deg^2 central region which has uniform *JK* data and reaches depths of $K_{AB} = 22.5$ and $J_{AB} = 22.5$ (5σ limits). By conducting simulations, the completeness at this magnitude limit is determined to be above 70 per cent for point sources. For details of the completeness estimation, image stacking, mosaicking and catalogue extraction procedures, see Foucaud et al. (2007). In addition to *J*- and *K*-band data from the UDS, deep *B* ($B_{\rm lim} = 28.2$), *V* ($V_{\rm lim} = 27.5$), *R* ($R_{\rm lim} = 27.6$), *i* ($i_{\rm lim} = 27.5$) and z'-band ($z'_{\rm lim} = 26.5$) data from the Subaru Suprimecam are also used (Sekiguchi et al. 2005).

The wealth of multi-band data available in this field, together with their depth and large area coverage, has enabled the construction of a highly detailed BzK colour–colour plot which displays many interesting features including a new branch (Fig. 1). For consistency the standard BzK definitions of Daddi et al. (2004), as discussed in the Introduction, were used to construct our BzK sample. *K*-band sources ($>5\sigma$) were cross-matched with our optical Subaru *i*-band source catalogue; since the Subaru field is not entirely coincident with the UDS field, this reduced the usable area. For *K*-band sources ($>5\sigma$) that did not have an optical match, 2 arcsec aperture magnitudes were obtained directly from the Subaru images. All BzK sources were then visually verified to make sure that they were not caused by diffraction spikes from saturated sources or cross-talk effects (Dye et al. 2006). Additionally, only sources that were not within the haloes of saturated optical sources were used, which left

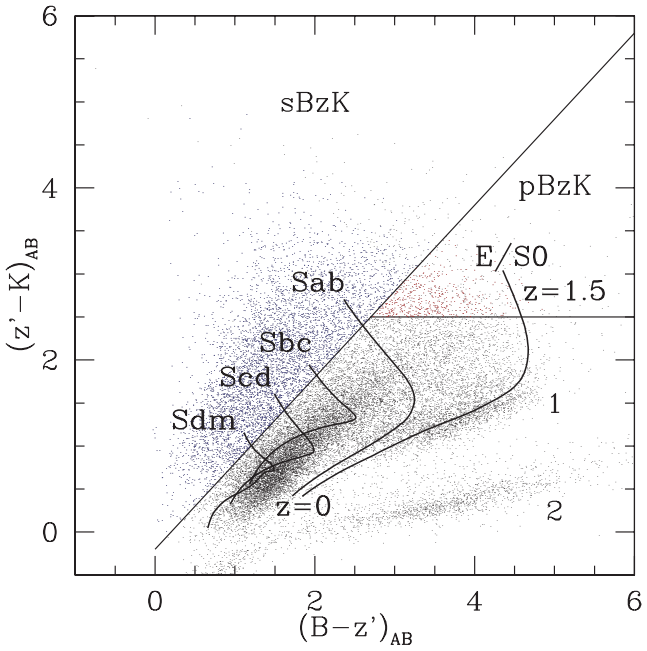

Figure 1. The BzK colour–colour diagram for sources in the UDS EDR. The sBzK and pBzK regions are marked accordingly. Branch 1 is the new branch of galaxies found in this study and Branch 2 is the stellar branch. Overlaid are no-evolution model tracks for a range of SED types, starting at $z = 0$ and ending at $z = 1.5$.

an area of 0.5591 deg^2. All *K*-matched sources were used for BzK selection unless both the *B*- and *z*-band magnitudes were $<1\sigma$ limits (0.7 per cent of the sample, outside saturated haloes), since these cannot be constrained within the BzK plane. This resulted in the selection of 6736 sBzKs and 816 pBzKs.

In addition to BzK selection, the availability of *R*- and *J*-band data in this field has also enabled the extraction of EROs and DRGs. In this case the ERO selection was defined as $(R - K)_{\rm vega} > 5.3$ and was carried out using the prescription presented in Simpson et al. (2006), resulting in 4621 EROs (to $K_{AB} = 22.5$). ERO selection was carried out independently because Simpson et al. (2006) used a different method of optical–near-infrared matching from that used here. The DRG sample used here was constructed by Foucaud et al. (2007) using a selection criterion of $(J - K)_{AB} > 1.3$, resulting in 369 DRGs (to $K_{AB} = 21.2$). Only those DRGs within the Subaru region and outside saturated haloes were used; this leaves 330 DRGs suitable for cross-matching with optical–near-infrared sources.

2.2 BzK number counts

The differential *K*-band number counts for the different populations in our survey (Fig. 2, Table 1) show that star-forming BzKs increase in number sharply toward fainter magnitudes. In contrast, pBzKs seem to exhibit a knee at $K \sim 21$ where the number counts clearly turn over before the limiting *K*-band magnitude; this feature is also seen in Kong et al. (2006). The small redshift range over which pBzKs are thought to be selected (Kong et al. 2006) could provide an explanation for the knee and the relatively faint magnitude at which pBzK number counts begin: that is, that the number counts are directly sampling the luminosity function of this population.

We note that the galaxies forming this knee feature have very faint *B*-band magnitudes, close to the completeness limit in this band ($B_{\rm lim} = 28.2$). However, fainter *B* magnitudes will push the

© 2007 The Authors. Journal compilation © 2007 RAS, MNRAS **379,** L25–L29

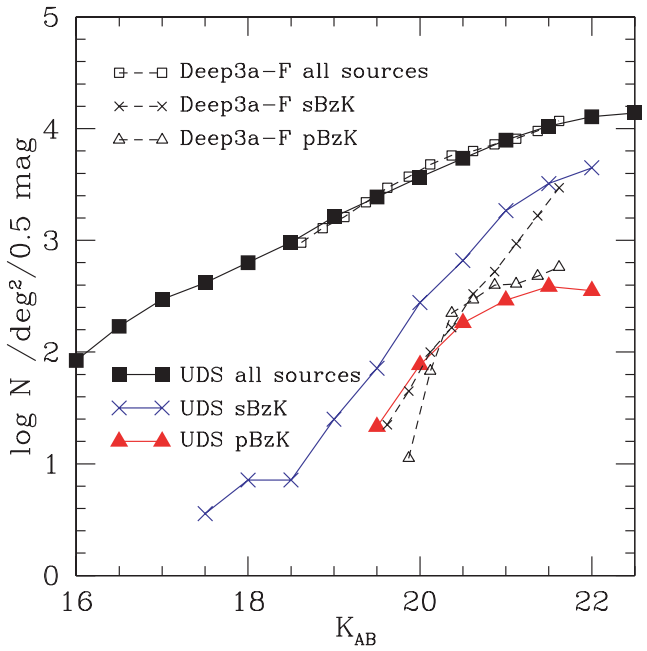

Figure 2. *K*-band differential number counts for all sources in the field and BzK sources. The sBzK population rises rapidly to our completeness limit, while the pBzK counts exhibit a knee at $K_{AB} \sim 21$. Data from the Deep3a-F sample of Kong et al. (2006) are included for comparison.

Table 1. Differential number counts in log [N deg^{-2} (0.5 mag)$^{-1}$] bins for sBzKs and pBzKs in the UDS EDR.

K bin centre	All sources	sBzK	pBzK
16	1.925	–	–
16.5	2.23	–	–
17	2.473	–	–
17.5	2.62	0.554	–
18	2.8	0.855	–
18.5	2.983	0.855	–
19	3.21	1.399	–
19.5	3.388	1.855	1.332
20	3.565	2.443	1.886
20.5	3.734	2.82	2.261
21	3.897	3.266	2.465
21.5	4.022	3.508	2.587
22	4.107	3.65	2.549

$B - z$ colours to the red and hence these sources should not be missed by our pBzK selection. At $K_{AB} \sim 21$ completeness is ∼100 per cent (Foucaud et al. 2007), so the feature is unlikely to be due to incompleteness. We conclude that this knee feature is likely to be real. We note that the turnover corresponds to absolute magnitude $M_K \sim 23.6$ at $z = 1.4$, which is close to the value of M^* determined for the *K*-band luminosity function at these redshifts (Cirasuolo et al. 2006).

As can be seen in Fig. 2, our results are similar in form to the data from the Deep3a-F survey (Kong et al. 2006), especially for the overall source number counts. However, for the sBzK number counts there is a slight magnitude offset, most likely due to cosmic variance. The UDS EDR has greater dynamic range in *K* because of our greater depth and area. This dynamic range will increase toward even fainter magnitudes with further UDS releases.

2.3 BzK new branch galaxies

Owing to the large number of detected sources in this survey field (34 098 in total), and the comparative depth of the optical data available, there are a large number of sources available for BzK analysis. It is clear from Fig. 1 (and also Fig. 4, later) that a new feature is visible running parallel with the stellar branch, at the bottom of the plot, but with redder $z' - K$ colour, roughly defined by the region

$$0.3(B - z') - 0.2 \lesssim (z' - K) \lesssim 0.3(B - z') + 0.4 \quad (1)$$

with clear branch separation at $(B - z') \gtrsim 2.5$.

Also plotted in Fig. 1 are no-evolution model tracks for different types of galaxy. These were created by redshifting SEDs from King & Ellis (1985), convolved with the appropriate filter response curve to get the relevant band magnitudes from which the $(B - z')$ and $(z' - K)$ colours can be calculated. The predicted track for early-type galaxies (E/S0) corresponds very well with the new branch of galaxies, especially at low redshifts. As can be seen, at higher redshift galaxies are no longer populating the predicted E/S0 model track. This is partly due to incompleteness at these high redshifts, but also because these model tracks do not take into account evolution, so early-type galaxies will be bluer at higher redshifts than the models predict. As such, they only provide a guide as to where different types of galaxies exist within the BzK plane. With greater depth (i.e. further data releases) this branch should fill out, and extend further towards the pBzK region, as larger numbers of passive galaxies, especially at high redshift, are included. The tracks of later type spirals fall predominantly within the main trunk of galaxies in the BzK diagram, and all lie within the sBzK region by $z \sim 1.5$. The proximity of the Sab model track to that of E/S0 suggests that there may be some contamination of the early-type branch by spirals, especially at low redshift.

3 ERO/BZK COMPARISON

The large number of EROs, BzKs and DRGs provided by the UDS EDR for the first time allows the overlaps between these populations to be analysed in detail. Previous studies have been made of the overlaps between EROs and BzKs, using smaller numbers of sources than are available here. Kong et al. (2006) find that 41 per cent of EROs are also selected as BzKs in their Deep3a-F data, and 29 per cent from their Daddi-F data. This compares with Daddi et al. (2004) who find that ∼35 per cent of their ERO-selected sources are also BzK-selected. In our much larger study we find that 60.6 ± 1.5 per cent of EROs (to $K_{AB} = 22.5$) are selected as BzK, of either variety, which is a higher fraction than found in previous studies. This is not surprising since the UDS EDR is deeper and contains fainter EROs, of which a larger fraction are likely to represent $z >$ 1.4 objects than would be expected in a brighter sample.

Fig. 3 shows the overlaps between the four populations studied here and the number of sources involved in each case. To ensure that we are only comparing samples to the same completeness depth, only EROs and BzKs selected to $K_{AB} = 21.2$ are used in this diagram, since this is the limit for DRG selection. However, when comparing EROs and BzKs we also quote numbers to a depth of $K_{AB} = 22.5$ in parentheses in the following discussion. As can be seen, 204(792) out of 214(816) pBzKs are additionally selected as EROs. The reason for this strong overlap is clear from the position of EROs on the BzK diagram (Fig. 4): EROs are located in a clearly defined region with red colours in $z' - K$ and $B - z'$ which covers the entire region occupied by pBzKs. It is also clear from Fig. 4 that sBzKs are far less preferentially selected as EROs –

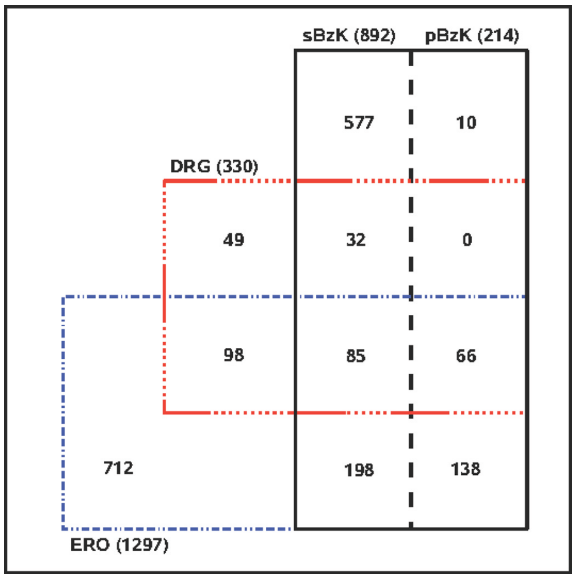

Figure 3. Venn diagram showing the overlaps in the number of objects classified as EROs, BzKs and DRGs. All numbers given here are to the depth of the DRG sample ($K_{AB} = 21.2$).

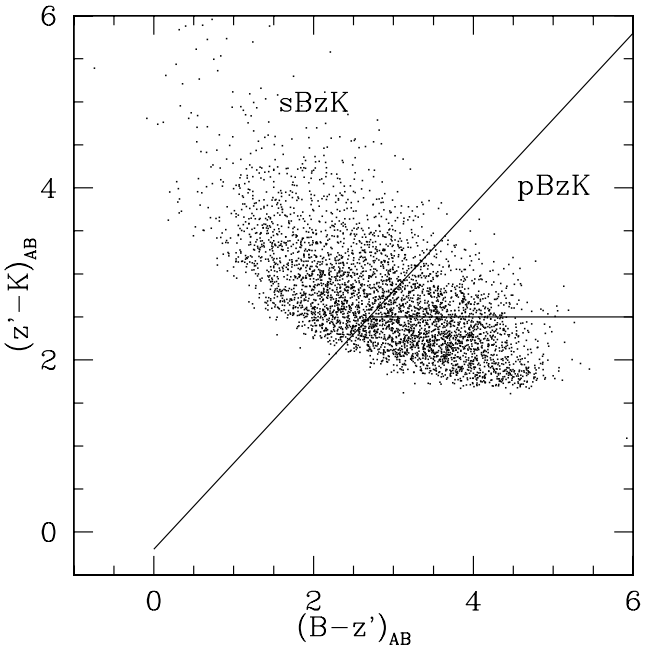

Figure 4. The BzK colours of EROs. Almost all pBzKs are EROs as well as a large fraction of sBzKs. This can also be seen in Fig. 3.

283(2007) out of 892(6736) sBzKs, or 31.7 ± 1.4 per cent(29.8 ± 1.2 per cent).

From the position of BzKs on a plot of $R - K$ colour versus K magnitude (Fig. 5) it can be seen that there is a clear difference in distribution between pBzKs and sBzKs. pBzKs have redder $R - K$ colour than sBzKs, with a narrow range around $R - K = 4.6$ (FWHM $\sim$ 0.24, see side panel in Fig. 5). This is in contrast to sBzKs which tend to be broad in $R - K$ colour but occupy regions with fainter K magnitude (see top panel in Fig. 5). This could be explained if sBzKs constitute the higher redshift ($z > 1.4$) end of the ERO population. The photo-z catalogue presented in Cirasuolo et al. (2006) shows the same redshift behaviour. However, given that these photo-z values are based on the same photometric data used here to construct the BzK population, and use the same SED features used to place galaxies at $z \sim 1.4$, this does not essentially add any new information, but serves as a consistency check.

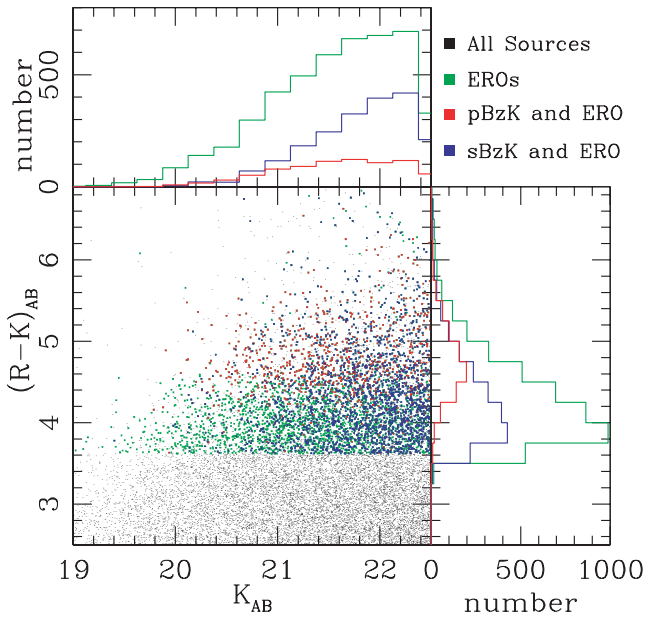

Figure 5. An $R - K$ diagram showing BzK-selected sources that are also selected as EROs. The histogram to the right shows the $R - K$ colour of EROs and ERO-selected pBzKs and sBzKs. It is clear that pBzKs have redder colours, whereas sBzKs cover a broad range in $R - K$ colour. The top histogram shows K-band aperture magnitudes for the same subsets. Much like the overall ERO population, sBzKs tend to be at higher magnitudes and peak around $K_{AB} \sim 22$; conversely, pBzKs have a much broader distribution which peaks at $K_{AB} \sim 21.2$.

4 DRG/ERO COMPARISON

The DRG selection technique was originally intended preferentially to select galaxies at $z > 2$. However, the most recent generation of large-area near-infrared surveys (e.g. Grazian et al. 2006; Conselice et al. 2006) are starting to probe the bright, low-redshift end of the DRG population. Based on photometric redshifts, Quadri et al. (2007) find > 70 per cent of DRGs (to $K_{vega} < 20$) from the Multiwavelength Survey by Yale–Chile (MUSYC) to lie at $z > 1.8$. Compared with the UDS EDR, however, the greater depth and substantially smaller area used in Quadri et al. (2007) mean that a much higher fraction of the DRGs selected are likely to lie at higher redshifts. A more comparable study is that of Conselice et al. (2006), in which a DRG sample is produced to a depth of $K_{vega} = 20.5$ over a slightly larger area than used in this study. They find their DRG sample to peak at $z \sim 1.2$, when using photometric redshifts, and at $z \sim 1.0$, when using spectroscopic redshifts, with only 4 per cent at $z > 2$. This redshift distribution does not change when their DRG sample is cut to the same depth as the DRG sample constructed in this study ($K_{vega} = 19.3$). We therefore take $z \sim 1.0$ also to be the likely redshift distribution of our DRG sample. A new picture is starting to emerge in which the DRG criterion selects not only $z > 2$ passive galaxies, but also galaxies at redshifts of $z \sim 1$. It is therefore interesting to see how DRGs cross-match with photometric populations of a more established nature, such as EROs and BzKs.

Most DRGs in the UDS EDR are also selected as EROs (75.5 ± 6.3 per cent, see Fig. 3). This means that these galaxies are red in both $R - K$ and $J - K$ colours which implies that they have a steep slope in their SEDs across this colour range. An SED feature of this kind at $z \sim 1$ is indicative of dusty star-forming galaxies or active galactic nuclei (AGN). *XMM–Newton* X-ray data are available for this field (Ueda et al., in preparation), but only six (1.8 ± 0.7 per cent) of our DRGs are found to be X-ray-detected. At the depth of the *XMM–Newton* data, however, this is only sufficient to rule out luminous AGN with relatively modest hydrogen column densities (e.g. $N_{\rm H} < 10^{23}{\rm cm}^{-2}$, assuming $L_X \simeq 10^{44}{\rm erg\,s}^{-1}$ at $z = 1.5$). Therefore the presence of highly obscured and/or lower luminosity AGN cannot be ruled out. Of the joint EROs and DRGs, 34.1 ± 4.3 per cent are sBzKs and 26.5 ± 3.7 per cent are pBzKs. The number of pBzKs in this overlap group suggests that a sizeable portion of these pBzKs are likely to be either obscured AGN or dusty star-forming galaxies rather than purely 'passive' pBzKs.

It would therefore appear that DRGs not only select $z > 2$ galaxies but also form part of the $z \sim 1$ ERO population, based in part on the DRG redshift determination from Conselice et al. (2006), as dust-reddened star-forming galaxies as well as a fraction of possible obscured AGN (see also Conselice et al. 2006).

5 DRG/BzK COMPARISON

Approximately half of the galaxies selected as DRGs are also selected as BzKs (117 sBzKs and 66 pBzKs). Although DRGs are selected as BzKs across the full DRG K magnitude and $J - K$ colour range, they tend to have fainter K magnitudes and are more efficiently selected by redder $J - K$ colours. Of these joint selections, 72.6 ± 10.4 per cent of the sBzK-selected DRGs were also selected as EROs, as were all of the pBzK-selected DRGs. This is as expected, because of the large fraction of DRGs selected as EROs (Section 4).

Reddy et al. (2005) find that ∼30 per cent of DRGs are found to be sBzKs, which is similar to the fraction of DRGs found as sBzKs in our study. Reddy et al.'s study also finds that ∼10 per cent of sBzKs are DRGs, as are ∼30 per cent of pBzKs; although sample errors will be high since only 17 pBzKs are used. This is in good agreement with this Letter which finds that 13.1 ± 1.3 per cent of sBzKs and 30.8 ± 4.3 per cent of pBzKs are also selected as DRGs. The large area of the UDS EDR data is probing the lower redshift, brighter end of the DRG luminosity function, so a large overlap with BzK-selected galaxies would be expected (we observe ∼55 per cent).

The larger fraction of pBzKs selected as DRGs could be due to the narrower and lower redshift range of pBzKs, as hypothesized in previous studies, combined with the DRG technique selecting galaxies at $z \sim 1$. It could also be due to some shared astrophysical feature, such as AGN (as discussed in Section 4). Whichever is correct, it is likely that BzKs constitute at least the $z \sim 1.4$–2.0 part of the DRG population. Those DRGs not selected as BzKs are likely to be at $z < 1.4$, as in Daddi et al. (2004), although some could be at $z > 2.5$.

6 CONCLUSIONS

For the first time a statistically significant study of the overlaps between ERO, BzK and DRG populations has been carried out. We compare 1297 EROs, 330 DRGs and 1106 BzKs, selected from 0.5591 deg^2 of imaging to $K_{AB} = 21.2$. It is found that BzKs are consistent with being the $z > 1.4$ end of the ERO population, as would be expected from the definition of these selection techniques.

It is becoming clear from the new generation of large-area surveys that the DRG selection criterion is effective at extracting not only high-redshift galaxies, but also dusty star-forming galaxies and obscured AGN, at $z \sim 1$, particularly at brighter K-band magnitudes ($K_{AB} < 22$). In this study we find that 249 of 330 DRGs are also selected as EROs. Those DRGs also selected as pBzKs tend to be at the red end of the DRG sample, while those also selected as sBzKs have a range in $J - K$ colour but are faint in K-band magnitude. This is consistent with DRGs selecting galaxies over a broad redshift range, from EROs at $z \sim 1$ to BzKs at $z \sim 1.5$. Deeper UDS data will also allow us to probe the faint end of the DRG selection regime to ascertain the effectiveness of this technique at selecting galaxies at $z > 2$.

The depth of our Subaru optical data has allowed us to determine the number–magnitude relations of the BzK samples. sBzKs have a broad range in magnitude, consistent with a broad range in redshift and/or luminosity. The pBzKs, however, exhibit a turnover in their number counts that is consistent with pBzKs inhabiting a narrow redshift range at $z \sim 1.5$. The UDS EDR combined with these Subaru data has also allowed the construction of the most complete BzK diagram yet seen. The number of sources has allowed the identification of a new feature that is most likely to be the no-evolution track of passive early-type galaxies with increasing redshift.

ACKNOWLEDGMENTS

This work is based partly on data obtained as part of the UKIRT Infrared Deep Sky Survey. We are grateful to the staff at UKIRT for making these observations possible. We also acknowledge the Cambridge Astronomical Survey Unit and the Wide Field Astronomy Unit in Edinburgh for processing the UKIDSS data. KPL, SF and CS acknowledge funding from PPARC. OA, IS and RJM acknowledge the support of the Royal Society. We thank the anonymous referee for comments which greatly improved the reliability of the results presented.

REFERENCES

Casali M et al., 2007, A&A, 467, 777
Cimatti A. et al., 2002, A&A, 381, L68
Cirasuolo M. et al., 2007, MNRAS, in press (doi:10.1111/j.1365-2966.2007.12038.x) (astro-ph/0609287)
Conselice C. J. et al., 2007, ApJ, 660, 55
Daddi E. et al., 2004, ApJ, 617, 746
Dye S. et al., 2006, MNRAS, 372, 1227
Foucaud S. et al., 2007, MNRAS, 376, L20
Franx M. et al., 2003, ApJ, 587, L79
Grazian A. et al., 2006, A&A, 453, 507
King C. R., Ellis R. S., 1985, ApJ, 288, 456
Kong X. et al., 2006, ApJ, 638, 72
Lawrence A. et al., 2007, MNRAS, in press (doi:10.1111/j.1365-2966.2007.12040.x) (astro-ph/0604426)
Quadri R. et al., 2007, AJ, submitted (astro-ph/0612612)
Reddy N. A. et al., 2005, ApJ, 633, 748
Roche N. D. et al., 2002, MNRAS, 337, 1282
Sekiguchi K. et al., 2005, in Renzini A., Bender R., eds, Multiwavelength Mapping of Galaxy Formation and Evolution. Springer, Berlin, p. 82
Simpson C. et al., 2006, MNRAS, 373, 21

This paper has been typeset from a TEX/LATEX file prepared by the author.

© 2007 The Authors. Journal compilation © 2007 RAS, MNRAS **379,** L25–L29